

Nghiên cứu đặc trưng cấu trúc và hoạt tính quang xúc tác phân hủy dung dịch RhB của vật liệu màng C/g-C₃N₄/PVDF

TÓM TẮT

Với tình trạng thiếu nước và khủng hoảng ô nhiễm toàn cầu, nhu cầu cấp thiết là phải phát triển các chất xúc tác quang mới hoạt động dưới ánh sáng khả kiến để làm sạch nguồn nước. Trong những thập kỷ qua, hầu hết các chất xúc tác quang được báo cáo đều ở dạng bột hoặc dạng hạt, gây khó khăn trong việc tách và tái chế. Để giải quyết những vấn đề này, một phương pháp đảo pha đơn giản đã được sử dụng để chế tạo vật liệu composite carbon/ graphit carbon nitride/ polyvinylidene fluoride (C/g-C₃N₄/PVDF) có cấu trúc dị thể. Vật liệu composite này sử dụng PVDF làm chất nền, tạo điều kiện thuận lợi cho việc loại bỏ và tách chất xúc tác quang khỏi dung dịch. So với g-C₃N₄ tinh khiết, vật liệu composite C/g-C₃N₄/PVDF mở rộng phạm vi hấp thụ ánh sáng của g-C₃N₄ về vùng ánh sáng khả kiến. Các chất mang được tạo ra do quang học được chuyển và tách hiệu quả trên chất nền carbon dưới sự chiết xạ của ánh sáng khả kiến, giúp tăng cường hoạt động quang xúc tác. Hơn nữa, vật liệu composite linh hoạt này cho thấy hiệu quả cao trong việc phân hủy thuốc nhuộm. Với chi phí thấp, khả năng tái sử dụng, hấp thụ ánh sáng khả kiến, dễ tổng hợp và hiệu suất quang xúc tác tuyệt vời, chất quang xúc tác này cho thấy tiềm năng to lớn trong các ứng dụng xử lý nước.

Từ khóa: composite, polyvinylidene fluoride, C/g-C₃N₄/PVDF, chất xúc tác quang, rhodamine B.

Study structure characteristics and the photocatalytic activities degradation of RhB solution on C/g-C₃N₄/PVDF membrane material

ABSTRACT

Given the global water shortage and pollution crisis, there is an urgent need to develop new photocatalysts that operate under visible light for water purification. Over the past decades, most the reported photocatalysts have been in powder or granular form, which caused difficulties in separation and recycling. To address these issues, a simple phase inversion method was employed to prepare a heterostructured carbon/graphite carbon nitride/polyvinylidene fluoride (C/g-C₃N₄/PVDF) composite. This composite uses PVDF as a substrate, facilitating the removal and separation of the photocatalyst from the solution. Compared with pure g-C₃N₄, the C/g-C₃N₄/PVDF composite extends the light adsorption range of g-C₃N₄ into the visible light region. The photogenerated carriers are efficiently transferred and separated on the carbon substrate under visible light irradiation, enhancing the photocatalytic activity. Furthermore, the flexible composite material demonstrates high efficiency in dye degradation. With its low cost, reusability, visible light absorption, ease of synthesis, and excellent photocatalytic performance, this photocatalyst shows great potential for water treatment applications.

Keywords: composite, polyvinylidene fluoride, C/g-C₃N₄/PVDF, rhodamine B, photocatalyst.

1. INTRODUCTION

In recent decades, photocatalysis has emerged as one of the most promising green technology thanks to its environmental benefits, cost-effectiveness, and high efficiency. It has found widespread applications in environmental management and energy conversion.^{1,2} A crucial aspect of advancing photocatalytic technology lies in developing new photocatalysts that can efficiently harness solar energy, addressing the pressing need for environmental remediation today.

In recent years, various technologies have been explored to develop effective methods for the complete removal of pharmaceutical compounds from water.^{3,4} Among these, advanced oxidation processes (AOPs) have been identified as a promising solution for treating difficult-to-degrade compounds. AOPs, particularly heterogeneous photocatalysis, have received significant due to their high efficiency in the removal of pharmaceuticals.^{5,6} Photocatalysts work by absorbing photons from an external light source to generate electron-hole pairs, which then participate in redox reactions. Among the various photocatalysts, graphitic carbon nitride (g-C₃N₄) has emerged as a promising metal-free, layered material that can be easily synthesized by thermal condensation

using inexpensive and abundant organic precursors in soil, such as urea.⁷

As a narrow band gap semiconductor (2.7 eV), g-C₃N₄ demonstrates stable physicochemical properties, excellent thermal stability, and remarkable photoelectron transfer capabilities. Additionally, it is non-toxic, easy to store, and can be obtained from various sources.⁸ Recently, g-C₃N₄ has become an optimal choice for forming heterostructured materials with wide-bandgap semiconductors. For example, Wang et al. developed a unique in situ microwave-assisted synthesis method to fabricate N-TiO₂/g-C₃N₄ composites, which showed significant improvements in photocatalytic activity.⁹ Similarly, Miranda et al. successfully obtained g-C₃N₄/TiO₂ composites with high photoactivity by the combination of hydrothermal and sintering methods, achieving a final phenol conversion rate of approximately 90%.¹⁰

However, recycling these materials after photocatalysis remains challenging.^{11,12} This not only leads to a significant waste of photocatalysts but also contributes to secondary environmental pollution. Several recovery methods for inorganic photocatalytic materials have been proposed, including the addition of magnetic materials, the creation of durable, recyclable, and flexible thin-film materials, and

their incorporation into organic polymer matrices.^{13,14}

Polyvinylidene fluoride (PVDF) is widely used for membrane fabrication, due to its high mechanical strength, chemical resistance, and thermal stability.^{15,16} Several g-C₃N₄-PVDF membranes have been developed and successfully applied in studies aimed at removing pollutants from water in continuous flow mode, with photocatalysts serving as self-cleaning materials that exhibit antifouling properties.^{17,18}

The main objective of this study is to modify the surface of PVDF membranes with g-C₃N₄. The performance of the modified membranes was evaluated in the degradation of Rhodamine B dye.

2. EXPERIMENTAL

2.1. Material synthesis

Chemicals: All chemicals used for material synthesis include Potassium hydroxide (KOH, 90%), Hydrochloric acid (HCl, 37%), Polyvinylidene fluoride (PVDF), N-Methyl-2-pyrrolidone (NMP) urea (CO(NH₂)₂, ≥99%) (Sigma-Aldrich) and rhodamine B (C₂₈H₃₁ClN₂O₃) Merck.

2.2. Materials synthesis:

2.2.1. Synthesis of C/g-C₃N₄

A mixture of urea (15 g) and C (0.1 g) was dispersed in a water-alcohol solution (1:1 ratio), then subjected to ultrasonic vibration for 30 minutes. The mixture was continuously stirred at 60 °C until the water and alcohol completely evaporated. The resulting solid was ground and heated in Argon gas at 550 °C for 1 hour. The product was then washed, filtered and dried at 80 °C for 12 hours to obtain the final product, denoted as C/g-C₃N₄.

2.2.2. Synthesis of C/g-C₃N₄/PVDF membrane material

To begin, add 0.1 gram of C/g-C₃N₄ material into a glass jar with a lid, then add 5 mL of N-Methyl-2-pyrrolidone (NMP). Sonicate the mixture for 10 minutes, followed by stirring for 30 minutes. Afterward, continue sonicating for another 20 minutes and stir for an additional 20 minutes. Next, add 0.646 grams of polyvinylidene fluoride (PVDF) and stir the mixture at 40 °C for 4 hours. Allow the mixture to stand for 3 hours. Use a stainless steel knife

(250 micrometres x 15 cm), evenly roll the mixture onto a glass surface to form a composite film. Quickly immerse the glass with the film into water to perform the phase inversion process.¹⁹ The resulting product is denoted as C/g-C₃N₄/PVDF.

The process for dispersing g-C₃N₄ onto PVDF polymer is carried out in a similar manner, and the product obtained is denoted as g-C₃N₄/PVDF.

2.3. Material characterization

The synthesized materials were characterized using several techniques. Infrared spectroscopy IR was performed on a Shimadzu IR Prestige-21. The crystal phase was analyzed by X-ray diffraction (XRD) using a Siemen D-500 Bruker system. Scanning electron microscopy (SEM) and X-ray energy dispersive spectroscopy (EDS) were conducted using a JSM-7600F device. Photoluminescence (PL) spectra were measured on a Hitachi F-7000 instrument with an excitation wavelength of 360 nm.

2.4. Photocatalytic evaluation

The photocatalytic activity of the obtained materials was evaluated by the decomposition of Rhodamine B (RhB) in an aqueous solution under visible light irradiation. A membrane containing 0.1 g of the photocatalyst was added to 100 mL of RhB solution with a concentration of 10 mg/L and stirred in the dark for 30 minutes to achieve adsorption-desorption equilibrium. The photocatalytic process was then initiated under a 30W LED light. Every 20 minutes, 5 mL of the solution was centrifuged to remove the solid part. The concentration of RhB in the solution was determined on a UV-Vis meter (CE-2011) at a wavelength of 553 nm.

3. RESULTS AND DISCUSSION

3.1. Material characteristics

XRD patterns were used to determine the crystalline phase of both g-C₃N₄/PVDF and C/g-C₃N₄/PVDF composites, as shown in Figure 1.

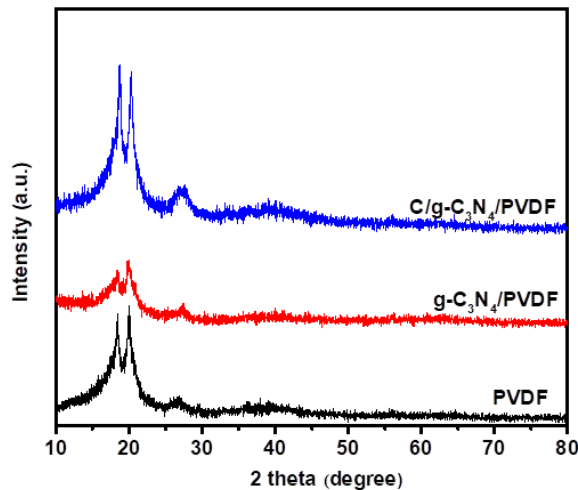


Figure 1. XRD patterns of PVDF, $g\text{-C}_3\text{N}_4$ /PVDF and $\text{C}/g\text{-C}_3\text{N}_4$ /PVDF.

PVDF is a semi-crystalline polymer with two main crystalline phases, α and β .^{20,21} The results in Figure 1 indicate three characteristic peaks at 18.5° , 20.1° and 26.7° , which are assigned to the reflection planes of (020), (110), and (021), corresponding to the α crystalline phase. When $g\text{-C}_3\text{N}_4$ or $\text{C}/g\text{-C}_3\text{N}_4$ were added to the PVDF polymer to form $g\text{-C}_3\text{N}_4$ /PVDF and $\text{C}/g\text{-C}_3\text{N}_4$ /PVDF composites, no significant change was observed compared to the pure PVDF sample. The three peaks attributed to the reflections of PVDF remain at nearly the same position but with varying intensities. In addition, the characteristic peak at 27.6° corresponding to the (002) plane of $g\text{-C}_3\text{N}_4$ appears in both the $g\text{-C}_3\text{N}_4$ /PVDF and $\text{C}/g\text{-C}_3\text{N}_4$ /PVDF samples in Figure 1. However, this peak is shifted and overlaps with the characteristic diffraction peak at 26.6° of PVDF. The peak at 27.6° corresponding to the (002) plane of $g\text{-C}_3\text{N}_4$ is believed to result from the alternating stacking of conjugated aromatic units, similar to the structure of graphite.²² The diffraction peaks of the $\text{C}/g\text{-C}_3\text{N}_4$ /PVDF composite are more intense than those of the $g\text{-C}_3\text{N}_4$ sample, likely due to the presence of carbon increasing the intensity of the peaks in this material sample.

FT-IR spectra were employed to characterize the chemical bond characteristics of the samples and the results are presented in Figure 2.

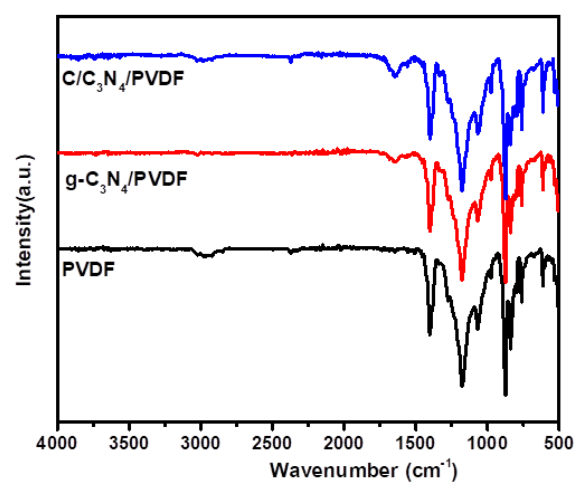


Figure 2. FT-IR spectra of PVDF, $g\text{-C}_3\text{N}_4$ /PVDF and $\text{C}/g\text{-C}_3\text{N}_4$ /PVDF.

The FTIR spectrum of the PVDF membrane shows that the peak at 763 cm^{-1} corresponds to the bending vibration of the CF_2 group. The peaks at 794 and 977 cm^{-1} are attributed to the shaking vibration of the CF_2 group, while the peak at 1170 cm^{-1} is associated with to be the valence vibration of the CF_2 group.^{23,24} The peak at 1413 cm^{-1} is deemed to be the valence vibration of the C-H functional group. In addition, the PVDF sample exhibits peaks at 875 , 615 , 531 , 490 cm^{-1} and all of which correspond to the α phase crystal structure of PVDF.²⁵ For the composite membrane materials $g\text{-C}_3\text{N}_4$ /PVDF and $\text{C}/g\text{-C}_3\text{N}_4$ /PVDF, the peak appearing at 1639 cm^{-1} is attributed to the valence vibration of the $\text{C}=\text{N}$ group.²⁶ The peaks at 2979 and 1411 cm^{-1} are assigned to the valence and deformation vibrations of the CH_2 group, respectively. In addition, the peak at 1181 cm^{-1} vibration is related to the valence vibration of the CF_2 group.²⁷

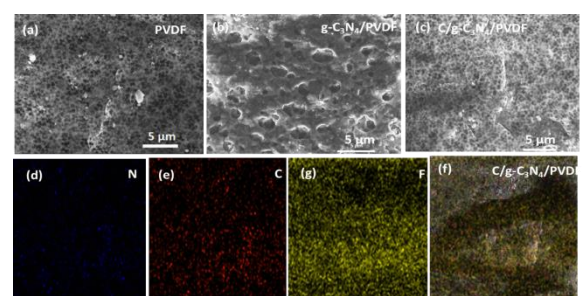


Figure 3. FE-SEM images of PVDF (a), $g\text{-C}_3\text{N}_4$ /PVDF (b), $\text{C}/g\text{-C}_3\text{N}_4$ /PVDF (c) samples, mapping images of $\text{C}/g\text{-C}_3\text{N}_4$ /PVDF (d) and N (d), C (e), F (g) material.

The SEM images reveal that the surface of pure PVDF (Figure 3.a) exhibits a homogeneous morphology. In comparison, the SEM image of $\text{g-C}_3\text{N}_4$ /PVDF (Figure 3.b) shows numerous voids between $\text{g-C}_3\text{N}_4$ and polymer chains, which are formed due to the particle distribution during the sample preparation. The SEM image of the C/g- C_3N_4 /PVDF composite (Figure 3.c) shows that many small particles are evenly dispersed on the PVDF substrate. These observations confirm that the voids between particles and polymer chains are influenced by the presence of carbon in the composite sample.²²

The EDX spectrum presented in Figure 4 was used to identify the elements present in the characterized C/g- C_3N_4 /PVDF composite film material.

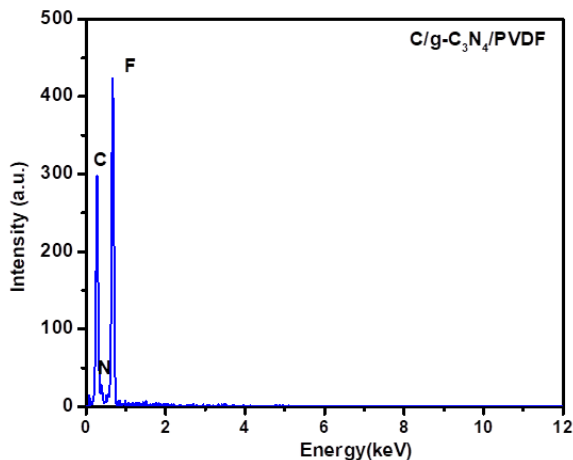


Figure 4. EDX spectrum of C/g- C_3N_4 /PVDF material.

The results in Figure 3d, c, f and Figure 4 confirm the presence of C, F, and N elements in the C/g- C_3N_4 /PVDF composite. As the photocatalytic activity of semiconductor materials is greatly affected by the recombination rate of photogenerated electron and hole pairs the photoluminescence (PL) spectrum is used to evaluate this recombination ability. The photoluminescence spectra of PVDF, $\text{g-C}_3\text{N}_4$ /PVDF and C/g- C_3N_4 /PVDF materials are presented in Figure 5.

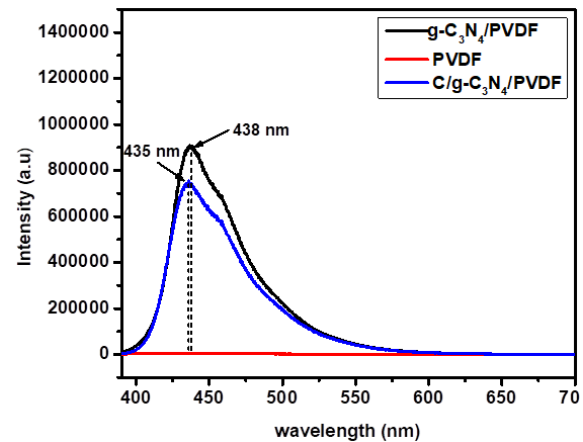


Figure 5. PL spectra of PVDF, $\text{g-C}_3\text{N}_4$ /PVDF and C/g- C_3N_4 /PVDF materials.

PL spectra of PVDF, $\text{g-C}_3\text{N}_4$ /PVDF and C/g- C_3N_4 /PVDF materials were conducted with excitation wavelength of 390 nm. As shown in Figure 5, the C/g- C_3N_4 /PVDF and C_3N_4 /PVDF show peaks at 435 and 438 nm, respectively. However, the C/g- C_3N_4 /PVDF material exhibits lower emission intensity compare to $\text{g-C}_3\text{N}_4$ /PVDF, which may be due to the addition of carbon helping improve the dispersion of the material. For PVDF membrane, no significant PL intensity is observed across the entire measured PL spectrum, indicating its limited adsorption properties. Consequently, the luminescence intensity is very low, nearly non-existent. Since PVDF does not have inherent luminescence, the observed PL shift is attributed to the excitation effect induced by the addition of $\text{g-C}_3\text{N}_4$ and carbon.²⁸ The PL spectral results suggest the recombination rate of electron-hole pairs in C/g- C_3N_4 /PVDF is lower than that in $\text{g-C}_3\text{N}_4$ /PVDF. This enhanced electron separation in C/g- C_3N_4 /PVDF creates favorable conditions for photogenerated electrons to diffuse to the catalyst surface where they interact with adsorbed H_2O or O_2 molecules to generate active free radicals, thus improving the efficiency of pollutant treatment.

3.2. Photocatalytic performance

The results of the photocatalytic evaluation for $\text{g-C}_3\text{N}_4$ /PVDF, C/g- C_3N_4 /PVDF, and C/g- C_3N_4 materials are shown in Figure 6. After 160 minutes of illumination, the RhB decomposition efficiency of the C/g- C_3N_4 /PVDF composite membrane reached 89%, which was higher than that of C_3N_4 /PVDF, C/g- C_3N_4 materials which achieved efficiencies of 45.92 and 82.97%, respectively. These results highlight the potential of $\text{g-C}_3\text{N}_4$ /PVDF, C/g- C_3N_4 /PVDF composite for practical membrane-based environmental treatment applications.

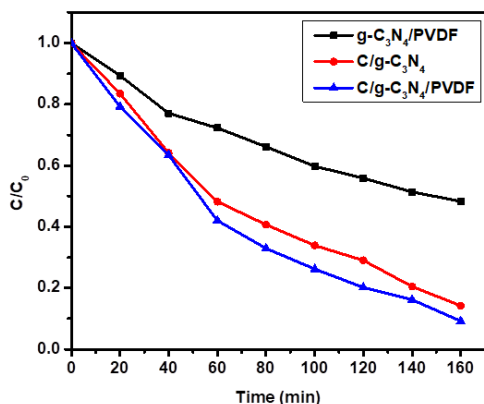


Figure 6. RhB decomposition under visible light of $g\text{-C}_3\text{N}_4/\text{PVDF}$, $C/g\text{-C}_3\text{N}_4$ and $C/g\text{-C}_3\text{N}_4/\text{PVDF}$ materials.

4. Conclusion

The phase inversion method was successfully used to synthesize $g\text{-C}_3\text{N}_4/\text{PVDF}$ $C/g\text{-C}_3\text{N}_4/\text{PVDF}$ materials. The obtained materials were characterized using modern physicochemical methods. XRD analysis clearly revealed the crystal phases while SEM images provided insight into the shape and dispersion of materials. The photocatalytic performance was evaluated through the decomposition of RhB solution, where the $C/g\text{-C}_3\text{N}_4/\text{PVDF}$ membrane demonstrated an impressive RhB decomposition efficiency of nearly 90%..

REFERENCES

1. K.N. Harish, H.S. Bhojya Naik, P.N. Prashanth Kumar, and R. Viswanath. Optical and photocatalytic properties of solar light active Nd-substituted Ni ferrite catalysts: for environmental protection, *ACS Sustainable Chemistry & Engineering*, **2013**, 1(9), 1143-1153.
2. J. Chen and C.S. Poon, Photocatalytic cementitious materials: influence of the microstructure of cement paste on photocatalytic pollution degradation, *Environmental science & technology*, **2009**, 43(23), 8948-8952.
3. J. Benner, D.E. Helbling, H.P.E. Kohler, J. Wittebol, E. Kaiser, C. Prasse, T.A. Ternes, C.N. Albers, J. Aamand, B. Horemans, and D. Springael. Is biological treatment a viable alternative for micropollutant removal in drinking water treatment processes?. *Water research*, **2013**, 47(16), 5955-5976.
4. D. Kanakaraju, B.D. Glass and M. Oelgemöller. Advanced oxidation process-mediated removal of pharmaceuticals from water: A review, *Journal of environmental management*, **2018**, 219, 189-207.
5. M. Antonopoulou, C. Kosma, T. Albanis, and I. Konstantinou. An overview of homogeneous and heterogeneous photocatalysis applications for the removal of pharmaceutical compounds from real or synthetic hospital wastewaters under lab or pilot scale, *Science of the total environment*, **2021**, 765(4), 144163-144245.
6. J. Meijide, G. Lama, M. Pazos, M.A. Sanromán, and P.S. Dunlop. Ultraviolet-based heterogeneous advanced oxidation processes as technologies to remove pharmaceuticals from wastewater: An overview. *Journal of Environmental Chemical Engineering*, **2022**, 10(3), 107630.
7. J. Wen, J. Xie, X. Chen, and X. Li. A review on $g\text{-C}_3\text{N}_4$ -based photocatalysts, *Applied surface science*, **2017**, 391, 72-123.
8. S. Zhou, Y. Liu, J. Li, Y. Wang, G. Jiang, Z. Zhao, D. Wang, A. Duan, J. Liu and Y. Wei, Facile in situ synthesis of graphitic carbon nitride ($g\text{-C}_3\text{N}_4$)- N-TiO_2 heterojunction as an efficient photocatalyst for the selective photoreduction of CO_2 to CO , *Applied Catalysis B: Environmental*, **2014**, 158, 20-29.
9. X.J. Wang, W.Y. Yang, F.T. Li, Y.B. Xue, R.H. Liu, and Y.J. Hao, In situ microwave-assisted synthesis of porous $\text{N-TiO}_2/g\text{-C}_3\text{N}_4$ heterojunctions with enhanced visible-light photocatalytic properties. *Industrial & Engineering Chemistry Research*, **2013**, 52(48), 17140-17150.
10. C. Miranda, H. Mansilla, J. Yáñez, S. Obregón and G. Colón, Improved photocatalytic activity of $g\text{-C}_3\text{N}_4/\text{TiO}_2$ composites prepared by a simple impregnation method, *Journal of Photochemistry and Photobiology A: Chemistry*, **2013**, 253, 16-21.
11. C. Yao, A. Yuan, H. Zhang, B. Li, J. Liu, F. Xi and X. Dong, Facile surface modification of textiles with photocatalytic carbon nitride nanosheets and the excellent performance for self-cleaning and degradation of gaseous formaldehyde, *Journal of colloid and interface science*, **2019**, 533, 144-153.
12. J. Zhao, J. Wang, L. Fan, E. Pakdel, S. Huang and X. Wang, Immobilization of titanium dioxide on PAN fiber as a recyclable photocatalyst via co-dispersion solvent dip coating, *Textile Research Journal*, **2017**, 87(5), 570-581.
13. C. Shi, J. Zhu, X. Shen, F. Chen, F. Ning, H. Zhang, Y.Z. Long, X. Ning and J. Zhao, Flexible inorganic membranes used as a high thermal safety separator for the lithium-ion battery, *Rsc Advances*, **2018**, 8(8), 4072-4077.
14. H. Liu, Z.G. Zhang, X.X. Wang, G.D. Nie, J. Zhang, S.X. Zhang, N. Cao, S.Y. Yan, and Y.Z. Long, Highly flexible $\text{Fe}_2\text{O}_3/\text{TiO}_2$ composite nanofibers for photocatalysis and ultraviolet detection, *Journal of Physics and Chemistry of Solids*, **2018**, 121, 236-246.

15. F. Yang, G.,Ding, J. Wang, Z. Liang, B. Gao, M. Dou, C. Xu and S. Li, Self-cleaning, antimicrobial, and antifouling membrane via integrating mesoporous graphitic carbon nitride into polyvinylidene fluoride. *Journal of Membrane Science*, **2020**, 606, 118146.

16. T.T. Zhou, F.H. Zhao, Y.Q. Cui, L.X. Chen, J.S. Yan, X.X. Wang and Y.Z. Long, Flexible $\text{TiO}_2/\text{PVDF}/\text{g-C}_3\text{N}_4$ nanocomposite with excellent light photocatalytic performance, *Polymers*, **2019**, 12(1), 55.

17. I. Kolesnyk, J. Kujawa, H. Bubela, V. Konovalova, A. Burban, A. Cyganiuk, W. Kujawski, Photocatalytic properties of PVDF membranes modified with $\text{g-C}_3\text{N}_4$ in the process of Rhodamines decomposition, *Separation and Purification Technology*, **2020**, 250, 117231.

18. J. Huang, J. Hu, Y. Shi, G. Zeng, W. Cheng, H. Yu, Y. Gu, L. Shi and K. Yi, Evaluation of self-cleaning and photocatalytic properties of modified $\text{g-C}_3\text{N}_4$ based PVDF membranes driven by visible light, *Journal of colloid and interface science*, **2019**, 541, 356-366.

19. L. Valenzuela, M. Pedrosa, A. Bahamonde, R. Rosal, A. Torres-Pinto, C.G. Silva, J.L. Faria and A.M. Silva, Carbon nitride–PVDF photocatalytic membranes for visible-light degradation of venlafaxine as emerging water micropollutant, *Catalysis Today*, **2023**, 418, 114042.

20. S. Vidhate, A. Shaito, J. Chung and N.A. D'Souza, Crystallization, mechanical, and rheological behavior of polyvinylidene fluoride/carbon nanofiber composites, *Journal of applied polymer science*, **2009**, 112(1), 254-260.

21. R. Song, D. Yang and L. He, Effect of surface modification of nanosilica on crystallization, thermal and mechanical properties of poly(vinylidene fluoride), *Journal of materials science*, **2007**, 42, 8408-8417.

22. L. Zhu, Y. Wang, F. Hu and H. Song, Structural and friction characteristics of $\text{g-C}_3\text{N}_4/\text{PVDF}$ composites, *Applied Surface Science*, **2015**, 345, 349-354.

23. N. Abzan, M. Kharaziha, S. Labbaf, Development of three-dimensional piezoelectric polyvinylidene fluoride-graphene oxide scaffold by non-solvent induced phase separation method for nerve tissue engineering, *Materials & Design*, **2019**, 167, 107636.

24. M. Kim, YS. Wu, EC. Kan, J. Fan, Breathable and flexible piezoelectric $\text{ZnO}@\text{ PVDF}$ fibrous nanogenerator for wearable applications, *Polymers*, **2018**, 10(7), 745.

25. KS. Tan, WC. Gan, TS. Velayutham, WH. Abd Majid, Pyroelectricity enhancement of PVDF nanocomposite thin films doped with ZnO nanoparticles, *Smart materials and structures*, **2014**, 23(12), 125006.

26. Y. Cui, L. Yang, M. Meng, Q. Zhang, B. Li, Y. Wu, Y. Zhang, J. Lang, C. Li, Facile preparation of antifouling $\text{gC}_3\text{N}_4/\text{Ag}_3\text{PO}_4$ nanocomposite photocatalytic polyvinylidene fluoride membranes for effective removal of rhodamine, *Korean Journal of Chemical Engineering*, **2019**, 36, 236-247.

27. N. Nikooe, E. Saljoughi, Preparation and characterization of novel PVDF nanofiltration membranes with hydrophilic property for filtration of dye aqueous solution, *Applied Surface Science*, **2017**, 413, 41-49.

28. Z. Vilamova, L. Svoboda, J. Bednar, Z. Simonova, R. Dvorsky, CG. Silva, JL. Faria, Enhancing photocatalytic $\text{g-C}_3\text{N}_4/\text{PVDF}$ membranes through new insights into the preparation methods, *Polymer*, **2024**, 127238-127249.